J Mater Sci (2010) 45:4705–4710
DOI 10.1007/s10853-010-4465-9

ULTRAFINE GRAINED MATERIALS

Comparison of deformation and microstructural evolution between equal channel angular pressing and forward extrusion using the dislocation cell mechanism-based finite element method

Soo-Hyun Joo · Hyoung Seop Kim

Received: 9 February 2010 / Accepted: 2 April 2010 / Published online: 15 April 2010

Abstract In order to compare plastic deformation and microstructural evolution behavior deformation between equal channel angular pressing (ECAP) and forward extrusion (FE) processes, finite element analyses in associated with the mechanism of dislocation glide and cell formation have been employed. It was found from the simulation results that the ECAP process is superior to the FE process, in terms of strength, grain refinement and deformation homogeneity as well as repeatability due to the equal channels of entry and exit.

Introduction

In recent years, several emerging methods have been proposed to produce ultrafine grained (UFG) or nanocrystalline bulk metallic materials by imposing severe plastic deformation (SPD) which can apply large shear strains [1–7]. It has been reported that materials with UFG microstructures show outstanding mechanical properties, such as high strength, high fatigue strength, good ductility, high strain rate and low temperature superplasticity, and high corrosion resistance. Equal channel angular extrusion/pressing (ECAE/ECAP), the most promising SPD technique, has been the subject of intensive studies in recent years due to its capability of producing fully dense UFG materials by repeated pressing of a workpiece through the L-shaped channel die having a channel angle Φ in the range of $75° <= \Phi <= 135°$. The unique characteristic of the SPD processes is their repeatability due to the same dimensions of the workpiece before and after the processes, which is inevitable for imposing giant strain. By a single pass of ECAP, one can obtain effective strain of ~ 1 under the generally used die condition of channel angle = 90° and corner angle = 20°.

Another well-known commercial metal forming process which can impose large plastic strain to bar- or rectangle-shaped long workpieces is extrusion [8–11]. The extrusion is a metal forming process in which a billet is forced to flow through a die whose exit diameter is smaller than that of the initial billet diameter. The billet flows through the die in the same direction (forward extrusion: FE) or opposite direction (backward extrusion: BE) as the punch either can be contained (high reductions) or open (low reductions) prior to entering the reduction portion of the die. Indeed, strain in a single pass of FE is similar to that in ECAP, e.g. average effective strain = ~ 0.75 under 50% area reduction ratio of frictionless FE. Although FE is able to generate a similar amount of strain by a single pass, it is not regarded as an SPD process because the final cross-section of the sample is smaller than the initial one and it cannot be repeated several times to assign a large strain, say 4–10.

Significant progress in analyzing the ECAP process itself as well as in understanding the fundamental properties of ECAP processed materials has been made using experimental and simulation approaches [3, 5, 7, 12–18]. In the numerical simulation approach, the finite element method (FEM) has been widely used for simulating materials and processing, such as the mechanical properties, and deformation homogeneity. Numerous authors have already analyzed the conventional ECAP [12–18] and the modified ECAP [19–21] as well as FE [22, 23] processes using FEM. Recently, FE has been merged with

---

S.-H. Joo · H. S. Kim (✉)
Department of Materials Science and Engineering,
POSTECH (Pohang University of Science and Technology),
Pohang 790-784, Korea
e-mail: hskim@postech.ac.kr

ECAP to further enhance the mechanical properties of the severe deformation processed materials [24, 25]. Although ECAP and FE have several similarities in qualitative grain refinement and strengthening, there are clear differences in deformation mode and quantitative aspects. Various SPD processing, such as ECAP, multi-axial compression/forgings and accumulative roll bonding (ARB) at room temperature, to approximately the same accumulated strain ($\sim$4) in Al 6061 alloy shows almost the same mechanical properties [26]. Nevertheless, there is no study on comparing the ECAP and FE processes, as far as the authors know. Moreover, it is widely said and believed, without any theoretical basis, that ECAP is not viable to be a commercially successful process due to a scale-up problem, while FE has no such a problem. There are only a few efforts for scaling-up of ECAP, e.g. Ref. [27]. Now at this stage of technical development, it is time to assess and compare the ECAP and FE processes.

The main object of the present paper is to compare the ECAP and FE processes in terms of plastic deformation using the theoretical simulation method of finite element. The processing loads are evaluated for assessing industrial aspect, and dislocation density and cell size are measured for microstructural aspect. The results and analysis will shed light on the scaling-up of ECAP in order to facilitate the application of ECAP in the industry as FE does.

Dislocation cell mechanism and the finite element method

For the comparison of the characteristics of deformation processing and microstructural evolutions, FEM simulations were carried out using the DEFORM 2D program package (Version 6.1) [28]. The standard constitutive model, such as stress versus strain data points, used in the simulations with FEM did not have a provision for accounting for microstructure development during plastic deformation. In the current simulations, a more advanced, deformation mechanism (dislocation theory) based constitutive model [14, 29–31] was utilized. It was specially designed for dislocation cell-forming materials undergoing large strain deformation. A good predictive capability of the model has been established in successful simulations of SPD of face-centered-cubic metals by ECAP. As the details of the model have been described elsewhere (cf. Refs. [29–31]), it is not presented here. It suffices to say the dislocation cell walls and cell interiors are treated as separated ‘‘phases,’’ with different dislocation densities, and that a ‘‘rule of mixtures’’ is used for calculating the stress in the ‘‘composite’’. The dislocation cell size is linked to the inverse of the square root of the total dislocation density calculated as a weighted sum of the dislocation densities in the cell walls and cell interiors. The model was shown to describe strain hardening behaviour of dislocation-cell forming metallic materials very well, including late stages of hardening. The simulations were carried out for the case of pure Cu using the model parameter values identified in Ref. [28, 29]: the initial grain size is 1 μm, and dislocation density is 7.75×10^7 mm^{-2}.

FEM simulations of plane strain ECAP and axisymmetric FE were carried out. Since the deformation mode in ECAP is plane strain, a hexahedron geometry is adequate to express this situation. On the other hand, an axisymmetric representation is necessary for FE of decreasing cross-sectional area. A hexahedron Cu specimen with dimensions of $10 \times 10 \times 60$ cm^3 was used for a preform in ECAP, as shown in Fig. 1a. The preform design slant at the back part of the workpiece head was applied, which is beneficial to homogeneous deformation, reducing the maximum pressing load at the initial stage and eliminating folding defects at strain concentration points [31]. The slant angle, channel angle, and corner angle were 45°, 90° and 0°, respectively. In order to compare processing loads of ECAP and FE, the sizes (i.e. cross-sectional area and volume) of the preforms need to be identical. For this purpose of objective comparison of the forming loads, an axisymmetric cylinder of initial radius $R_o = 5.64$ cm, which represents the same cross-sectional area of 100 cm^2 as that of ECAP, was used for FE. In addition to the preform size factor, the reduction ratio in FE is an important factor for industrial applicability. For comparing the deformation and microstructural characteristics of two processes, the same preform size and processing load should be kept. That is, a

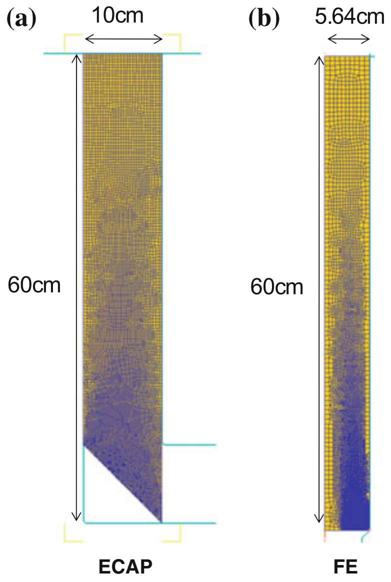

Fig. 1 Preform geometries and initial mesh systems for FEM simulations of ECAP and FE. The two preforms have the same cross-sectional area of 100 cm^2

process generating high and homogeneous deformation is preferred under the same loading conditions, and a process of a low processing load is preferred among processes developing the same strains. To find the reduction ratio in FE generating the same load in ECAP, three exit radii $R_f = 4.89$ cm, $R_f = 4.72$ cm and $R_f = 4.55$ cm with corresponding area reduction ratios of 25%, 30% and 35%, respectively, were used for FE. The half die angle was 45°.

The number of initial meshes of 4-noded elements was 10,000 for both ECAP and FE. This number of elements was found to be sufficient to express local deformation of the materials through calculations with varying number of elements. Die and punch were modeled as rigid parts. A temperature effect of the sample and die was ignored. The friction factor between the inner surfaces of the dies and the specimens was assumed to be 0.1, a typical cold metal forming value. All simulations were carried out at a constant punch speed of 1 mm/s.

Results and discussion

Figure 2 represents the predicted processing loads versus punch moving time in ECAP and FE. The ECAP load in the back slant preform case (dashed curve in Fig. 2) clearly shows two-stage behavior: load increasing and steady stages, without overshoot which is common (about 15% of the ECAP load) in the convention hexahedron preform ECAP. In stage I, as the head part of the workpiece goes through the main deformation zone, the load increases because the strain and the volume of the deformation part of the workpiece increase. It should be noted that plastic flow is smooth in Fig. 3a, and no strain concentration point is found in the deformed workpiece. Stage II commences after the load reaches a steady state load of ~2500 kN. Since there is no load overshoot, the full load capacity of the press machine can be utilized for entire workpiece forming, and thus ~15% scale-up of the ECAP process can be realized with the same press machine. The predicted loads in FE of 25, 30, and 35% area reduction ratios are 2100, 2500 and 2800 kN, respectively. From these simulations it is found to be possible to process ECAP of 90° channel angle and FE of 30% area reduction of an initial 100 cm^2 cross-section specimen using a 2500 kN pressing machine. Indeed, a press machine of 2500 kN capacity is widely used for extrusion in mechanical and machinery industries, hence FE presses can be applied for ECAP without a power problem.

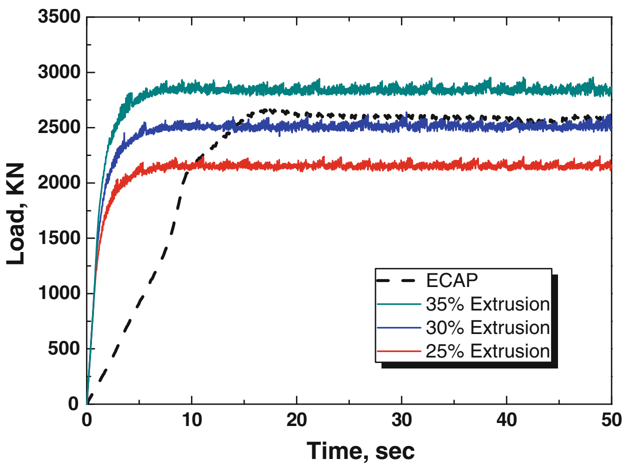

Fig. 2 Operating load versus time curves

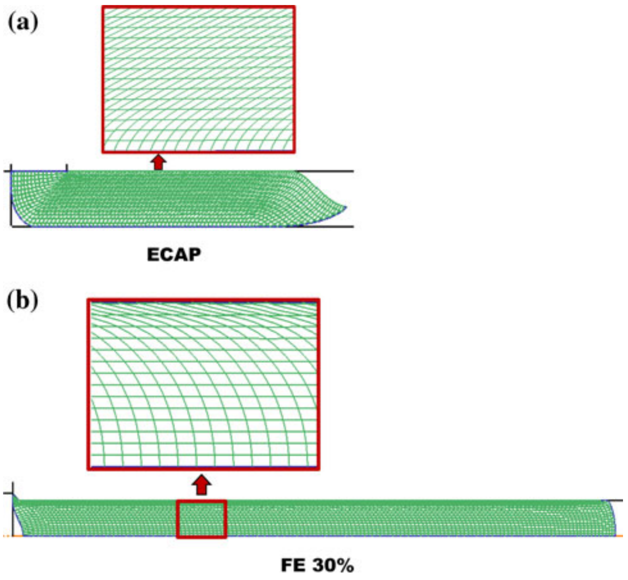

Fig. 3 Deformed geometries and flow nets after finishing ECAP and FE of 30% area reduction

The deformed geometries and flow nets of the ECAP and FE of 30% area reduction after finishing the processing are shown in Fig. 3. The mode of deformation in the ECAP is almost simple shear except the bottom region where the deformation mode is a mixture of simple shear and rigid body rotation due to the corner gap formation, see Fig. 3a. It is well established that the corner gap is generated by the effect of the strain hardening property [32–34]. The flow pattern in FE of 30% reduction shown in Fig. 3b is more nonuniform than that in ECAP, i.e. highly sheared in surface region and compressed in radial direction without shearing in the central region. As the extrusion ratio increases, the flow nets become more distorted at the surface as compared to the center of the die. Along the extrusion direction, the head region is similar to the central steady region, but the piping phenomenon was observed in the tail region.

Quantitative comparisons for deformation can be made from the effective plastic strain distribution in Figs. 4 and 5. It can be observed that the uniform deformation compared to the cases of FE was attained in ECAP samples.

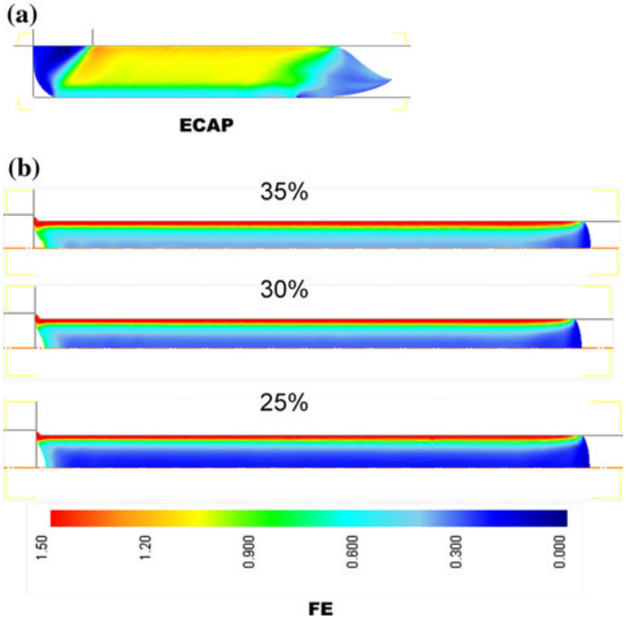

Fig. 4 Effective plastic strain distributions for **a** ECAP and **b** FE of various area reduction ratios

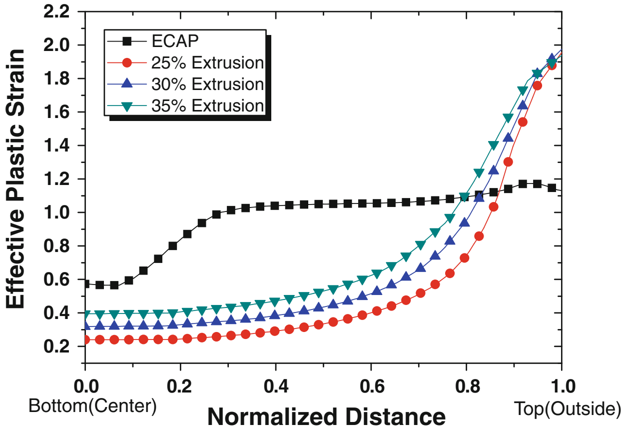

Fig. 5 Effective plastic strain path plots from bottom to top of the processed samples

The samples processed by FE show nonuniform deformation along the radial direction with more deformation in the outer region than the center. Deformation in the surface region is due to the flow constraint by the die corner and the friction effect, hence the half die angle is an important factor for surface deformation. On the other hand, deformation except in the surface region is determined by the reduction ratio. Therefore, it can be observed that the deformation increases with the area reduction of area except the surface region where developed strains are the same in all cases. Numeric values of strain can be cleared compared in Fig. 4: effective plastic strain is minimum of ∼0.6 in the bottom and maximum of ∼1.2 in the top region in ECAP. Average values of effective strain are 0.98, 0.77, 0.89 and 1.0 for ECAP and 25%, 30% and 35% area reduction FE, respectively. That is, the average plastic strain ($\varepsilon = 0.98$) developed in ECAP is higher than that ($\varepsilon = 0.89$) in FE under the same preform and pressing load condition, which means more severe plastic deformation and grain refinement can be achieved using ECAP than FE. Moreover, ECAP is superior to FE in terms of deformation homogeneity, in that ECAP can generate more homogeneous strain distribution than FE, as can be seen in the strain distribution chart of Fig. 6. ECAP shows the homogeneous strain of narrow distribution, while FE has a wide plastic strain distribution.

Microstructural evolutions, such as dislocation density and cell size, are directly related to the amount of plastic strain; hence, the results of dislocation density distributions can be expected easily, as shown in Figs. 7 and 8. The higher plastic strain is applied, the more dislocations are generated, which produces the same distributions of

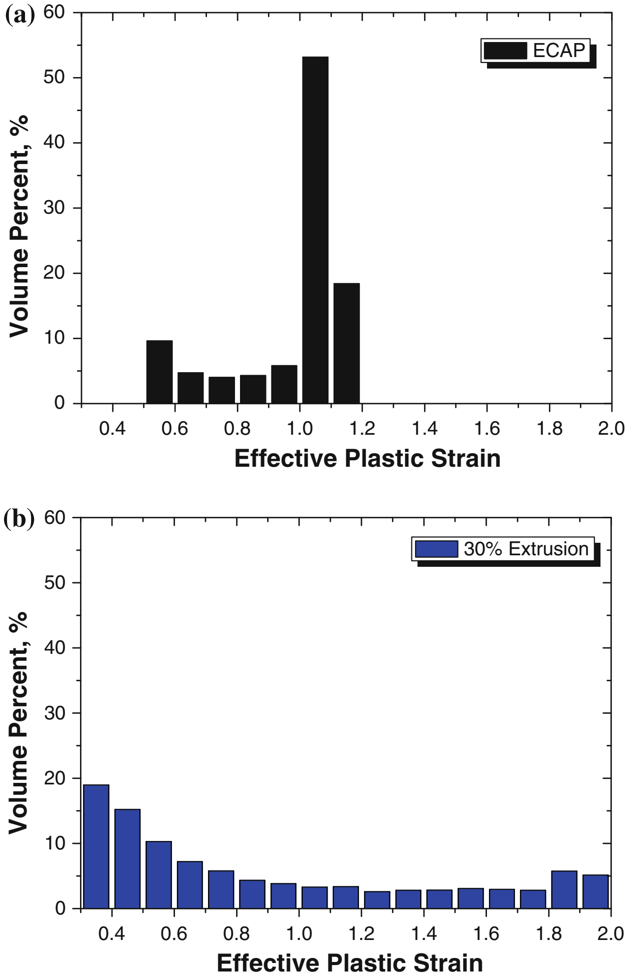

Fig. 6 Effective strain distributions for **a** ECAP and **b** FE of 30% area reduction ratio

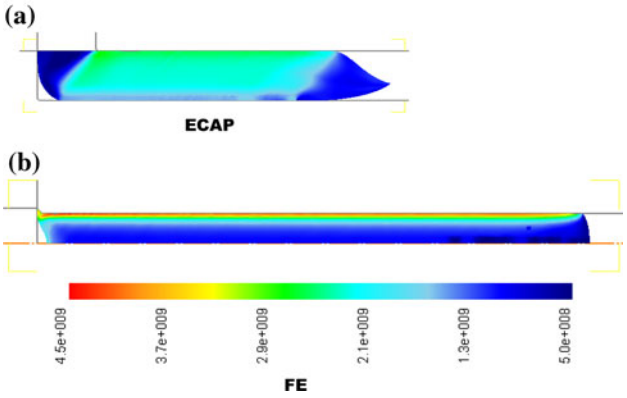

Fig. 7 Dislocation density distributions for **a** ECAP and **b** FE of 30% area reduction ratio

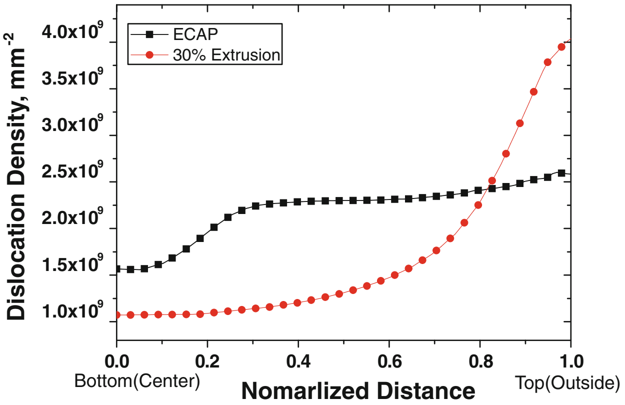

Fig. 8 Effective strain path plots from bottom to top of the processed samples

dislocation density as plastic strain. The average dislocation densities are 2.20×10^9 mm^{-2} and 2.13×10^9 mm^{-2} in ECAP and FE of 30% area reduction. Strength of the ECAP processed Cu is expected to be more uniform and higher than that of the FE sample, because stress is proportional to square root of dislocation density.

Likewise, the predicted cell size is smaller and more uniform in ECAP than in FE, see Figs. 9 and 10. The average cell/grain sizes are 189 and 205 nm, respectively, in ECAP and FE processed Cu. ECAP can be employed to obtain higher strength and grain refinement than FE. Therefore, it can be concluded that ECAP is superior in terms of strain development and strain homogeneity to FE under the same pressing loads and preforms.

Conclusions

Comparison of ECAP and FE of Cu has been studied by the finite element method implemented with the deformation mechanism-based constitutive model to find out the plastic deformation and microstructural evolution during the processing. The deformation mechanism considered is dislocation mechanism forming dislocation cell structures. It was possible to process ECAP of 90° channel angle or FE of 30% area reduction of the same preforms using the same power pressing machine. Hence, FE presses can be applied for ECAP without a power shortage problem which is the bottle neck for scaling-up, using ECAP tooling in a conventional press, contrary to general expectation. ECAP is superior to FE in that more severe plastic deformation, higher strength and more grain refinement can be achieved using ECAP than FE. Moreover, ECAP can generate more homogeneous strain distribution than FE. It is the belief of the authors that ECAP should be applied to the up-scaled engineering parts of UFG/nanocrystalline microstructured metallic materials in a near future.

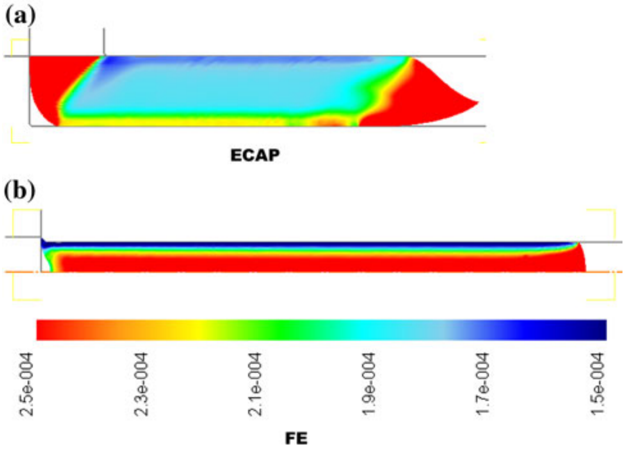

Fig. 9 Effective strain distributions for **a** ECAP and **b** FE of various area reduction ratios

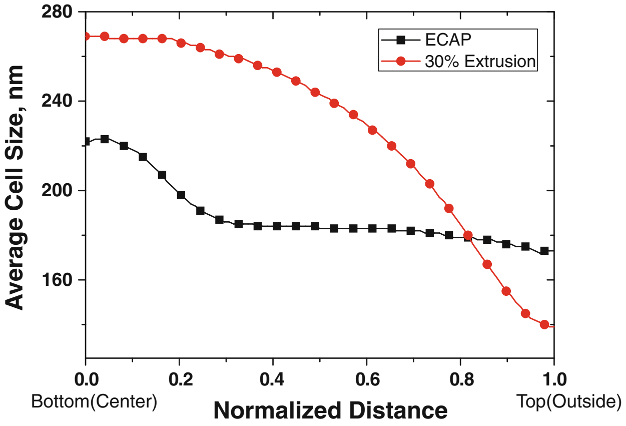

Fig. 10 Effective strain path plots from bottom to top of the processed samples

Acknowledgements This research was supported by a grant from the Center for Advanced Materials Processing (CAMP) of the 21st Century Frontier R&D Program funded by the Ministry of Knowledge Economy, Republic of Korea. The calculations were performed using the supercomputing resources of the Korea Institute of Science and Technology Information (KISTI). SHJ was supported by the second phase of the Brain Korea 21 Program in 2010.

References

1. Valiev RZ, Islamgaliev RK, Alexandrov IV (2000) Prog Mater Sci 45:103
2. Valiev RZ, Estrin Y, Horita Z, Langdon TG, Zehetbauer MJ, Zhu YT (2006) JOM 58:33
3. Valiev RZ, Langdon TG (2006) Prog Mater Sci 51:881
4. Kim HS, Estrin Y (2001) Appl Phys Lett 79:4115
5. Kim HS, Ryu WS, Janecek M, Baik SC, Estrin Y (2005) Adv Eng Mater 7:43
6. Jang YH, Kim SS, Han SZ, Lim CY, Goto M (2008) Metal Mater Int 14:171
7. Segal VM, Reznikov VI, Drobyshevskiy AE, Kopylov VI (1981) Russ Metall Transl 1:99
8. Chen DC, Syu SK, Wu CH, Lin SK (2007) J Mater Process Tech 192–193:188
9. Blazynski TZ (1971) Int J Mech Sci 13:113
10. Lee CS, Caddell RM, Yeh GSY (1972) Mater Sci Eng 10:241
11. Azeem MA, Tewari A, Mishra S, Gollapudi S, Ramamurty U (2010) Acta Mater 58:1495
12. Prangnell PB, Harris C, Roberts SM (1997) Scr Mater 37:983
13. Kim HS (2001) J Mater Process Tech 113:617
14. Baik SC, Estrin Y, Hellmig RJ, Jeongc HT, Brokmeier H-G, Kim HS (2003) Z Metallkd 94:1189
15. Moon BS, Kim HS, Hong SI (2002) Scr Mater 46:131
16. Han J-H, Chang H-J, Jee K-K, Oh KH (2009) Metal Mater Int 15:439
17. Yoon SC, Nagasekhar AV, Kim HS (2009) Metal Mater Int 15:215
18. Nagasekhar AV, Kim HS (2009) Metal Mater Int 14:565
19. Kim HS (2009) Mater Sci Eng A 503:130
20. Nagasekhar AV, Kim HS (2008) Metal Mater Int 14(5):565
21. Nagasekhar AV, Kim HS (2008) Comput Mater Sci 43:1069
22. Lee CM, Yang DY (2000) Int J Mach Tools Manufac 40:33
23. Hambli R (2009) Finite Elem Anal Des 45:6404
24. Nagasekhar AV, Yoon SC, Yoo JH, Kang S-Y, Baik SC, Kim HS (2010) Mater Trans, submitted
25. Zi A (2010) Mater Character 61:141
26. Cherukuri B, Nedkova TS, Srinivasan R (2005) Mater Sci Eng A 410–411:394
27. Chaudhury PK, Cherukuri B, Srinivasan A (2005) Mater Sci Eng A401–411:316
28. DEFORM 2D software, http://www.deform.com
29. Baik SC, Estrin Y, Kim HS, Hellmig RJ (2003) Mater Sci Eng A351:86
30. Baik SC, Hellmig R, Estrin Y, Kim HS (2003) Z Metallkd 94:754
31. Estrin Y, Kim HS (2007) J Mater Sci 42:1512. doi:10.1007/s10853-006-1282-2
32. Yoon SC, Seo MH, Kim HS (2006) Scr Mater 55:159
33. Şimşir C, Karpuz P, Gür CH (2010) Comput Mater Sci, submitted
34. Kim HS, Seo MH, Hong SI (2000) Mater Sci Eng 291A:86